Book of Tutorials and Abstracts

European Microbeam Analysis Society

EMAS 2019

16th

EUROPEAN WORKSHOP

on

MODERN DEVELOPMENTS AND APPLICATIONS IN MICROBEAM ANALYSIS

19 to 23 May 2019
at the
NTNU, Realfagbygget
Trondheim, Norway

Organised in collaboration with:
Norwegian University of Science and Technology
(NTNU)

EPMA, RAMAN AND XANES APPLIED FOR THE STUDY OF OXIDATION PROCESSES IN GLASS

Ery C. Hughes[1], B. Buse[1], S.L. Kearns[1], R. Brooker[1], D. di Genova[2], G. Kilgour[3], H. Mader[1] and J. Blundy[1]

1 University of Bristol, School of Earth Sciences
Wills Memorial Building, Queens Road, Bristol BS8 1RJ, Great Britain
2 Technische Universität Clausthal, Institut für Nichtmetallische Werkstoffe
Zehntnerstrasse 2a, 38678 Clausthal-Zellerfeld, Germany
2 GNS Science, Wairakei Research Centre
114 Karetoto Road, RD4, 3384 Taupo, New Zealand
e-mail: ery.c.hughes@gmail.com

Ery Hughes studied Natural Sciences (B.A.), specialising in Earth Sciences (MSc), at the University of Cambridge, and then completed her PhD at the School of Earth Sciences, University of Bristol. Her Master's research project combined multi-scale 3D X-ray μ-tomography and 2D high-resolution SEM to understand the fragmentation process in pantellerite magmas, which are low viscosity melts able to fragment in a brittle fashion. Her PhD focussed on developing and combining various microanalytical techniques for the analysis of volcanic rocks to quantify the H_2O, CO_2, and Fe oxidation state of melts prior to eruption, with a particular focus on using EPMA and SIMS.

1. ABSTRACT

Quantifying the oxidation state of Fe and S in silicate melts is an important aspect of volcanology and igneous petrology as the ratios can be used as proxies for oxygen fugacity, a fundamental thermodynamic parameter that provides information on the chemical history of melt from the magma chamber to the Earth's surface. In practice, analyses of these elements are performed on quenched volcanic melt forming the matrix between crystals or as trapped inclusions. As a result, microanalytical techniques are required due to their small volume and multiple techniques are applied to the same small region to extract the full information required to understand volcanic and magmatic processes. This can be problematic as glasses are often unstable under the electron and photon beams used to analyse them. It is, therefore, important to understand the compositional and structural changes to the glass during analysis to ensure accurate measurements and that subsequent complimentary analyses are not compromised. Here we look at the most common techniques currently used for measuring the oxidation state of Fe and S in silicate glass and how these glasses respond to electron and photon beam irradiation.

2. INTRODUCTION

Volcanoes predominantly erupt silicate melts carrying crystals and bubbles in a wide range of eruptive styles, from effusive lava flows to explosive Plinian eruptions. Understanding the controls on eruption style, and methods to predict eruption style from volcano monitoring data, are key to reducing the risk posed by volcanoes. This requires quantifying the parameters that affect the chemical and physical properties of the magma. Natural melts cover a wide range of compositions, containing ~ 45 - 75 wt% SiO_2 and varying amounts of TiO_2, Al_2O_3, Fe_2O_3/FeO, CaO, MgO, MnO, Na_2O, K_2O, and P_2O_5 (Fig. 1). Additionally, silicate melts contain volatiles such as H_2O, CO_2, S, and halogens. There are two main compositions discussed here (Fig. 1): basaltic glasses are low-silica (~ 50 wt% SiO_2), Fe-rich (~ 10 wt% FeO), and alkali-poor (< 5 wt% Na_2O+K_2O) glasses; whilst rhyolitic glasses are high-silica (~ 70 wt% SiO_2), Fe-poor (~ 3 wt% FeO, except pantellerites which contain ~ 8 wt% FeO), and alkali-rich (~ 8 wt% Na_2O+K_2O) glasses.

Oxygen fugacity (fO_2) is equivalent to the partial pressure of oxygen in a system, and is a key thermodynamic parameter, which controls the oxidation state of multivalent elements within the magma (e.g., mainly Fe and S, but also potentially Mn, Cr, V, Ce, and Eu; [1-3]). Figure 2 illustrates how fO_2 controls the valency of Fe and S, which can have a major effect on the physical and chemical properties of the magma. The fO_2 affects volatile solubility, crystallisation (e.g., phase assemblage), and magma viscosity, as well as controlling the composition of exsolved vapour and even the secondary formation of economic ore bodies (e.g., [4-9]). The fO_2 varies between different magmatic systems, often related to tectonic setting, but can also be perturbed by processes such as fractionation and degassing (e.g., [10, 11]). For these reasons it is an important parameter to constrain when investigating the evolution of magmatic systems, as

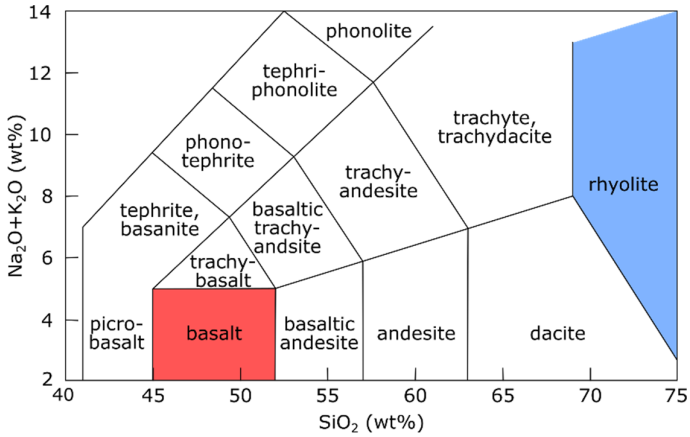

Figure 1. TAS plot (total alkalis, Na_2O+K_2O, against silica, SiO_2) with the different rock types labelled. The two main glass compositions discussed here are highlighted: basalt (red) and rhyolite (blue).

it can have an important impact on eruption dynamics. It has recently been suggested that decompression can induce the formation of magnetite (or haematite) nanocrystals called "nanolites" (particles as small as 30 nm in size [12]). This may also be related to how the oxidation state of the melt changes due to degassing during ascent [13].

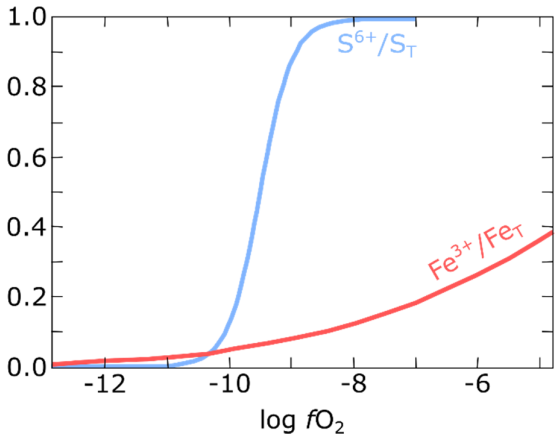

Figure 2. Effect of oxygen fugacity (fO_2) on melt Fe (Fe^{3+}/FeT) and S (S^{6+}/ST) oxidation state from [1] and [14], respectively.

Understanding the importance of these processes requires some estimate of the magma oxidation state prior to eruption, which can be deduced by measuring the Fe or S oxidation state of the melt. One common way to do this is by analysing melt inclusions (tiny pockets of glass 1 – 500 µm in diameter found in crystals) or matrix glass (final melt composition) (Fig. 3). Melt inclusions form when melt becomes trapped during crystal growth, which provides a unique sample of the melt prior to eruption [15].

Multiple microanalytical techniques are often used to analyse melt inclusions and matrix glass due to the wide variety of elements present (at variable concentrations) and range of information required (e.g., concentration, oxidation state, isotope ratio, etc.). This means that the same area

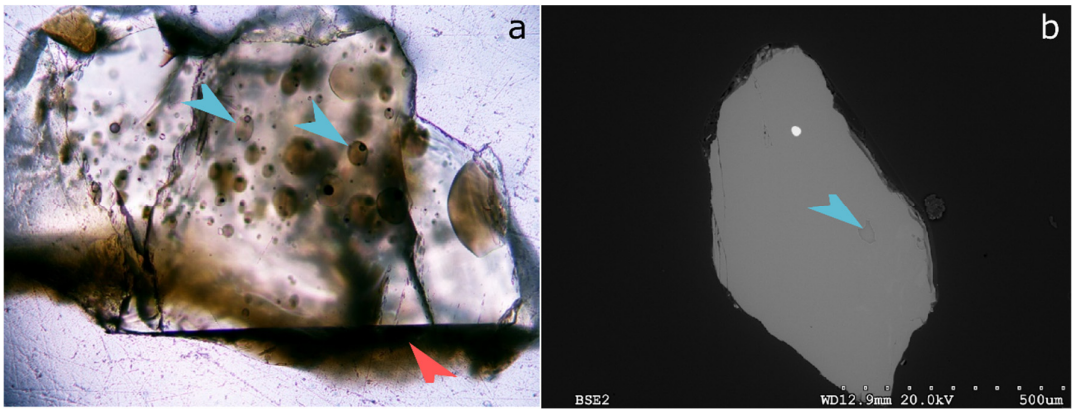

Figure 3. a) Transmitted light photomicroscope image of an olivine crystal from Stromboli (Italy) containing melt inclusions (blue arrow, often containing smaller, circular, black bubbles) and brown matrix glass (red arrow). b) Back scattered electron image of a pyroxene crystal from Tarawera (New Zealand) containing a melt inclusion (blue arrow).

of glass may be analysed many different times. Typical options are electron probe microanalysis (EPMA) for major/minor element concentrations; laser-ablation inductively-coupled plasma mass spectrometry (LA-ICP-MS) for trace element concentrations; Fourier-transform infrared spectroscopy (FTIR) for volatile concentrations and speciation; Raman spectroscopy for melt structure and H_2O concentration; secondary ion mass spectrometry (SIMS) for volatile/trace element concentrations and isotope ratios; and more recently X-ray absorption near-edge structure (XANES) spectroscopy for oxidation state. As a result, it is important to understand if, and to what extent, these measurements affect the glass to understand whether subsequent analyses are being compromised.

3. *TECHNIQUES FOR ANALYSING GLASS OXIDATION STATE*

Iron occurs naturally as Fe^{2+} and Fe^{3+} in silicate glass and the Fe oxidation state (Fe^{2+}/FeT) can be analysed using a variety of microanalytical techniques [16] (Fig. 4). Listed in order of decreasing analysis area, these include: EPMA (~ 20 - 60 µm in diameter, [17-19]), µ-Mössbauer (~ 5 × 10 µm, [20]), µ-XANES spectroscopy (~ 2 × 2 µm, [21]), Raman spectroscopy (~ 1 µm in diameter, [22, 23]), and EELS (electron energy-loss spectroscopy, [24]). Sulphur occurs as S^{2-} and S^{6+} in natural silicate glass and generally has a much lower concentration than Fe (< 5,000 ppm S versus 4 - 15 wt% FeO), but the oxidation state (S^{6+}/ST) can also be analysed in silicate glass using EPMA (~ 50 μm^2, [25]) or µXANES (~ 0.3 × 0.3 µm, [26]). However, some of these techniques can cause beam damage during analysis, as discussed in the following section.

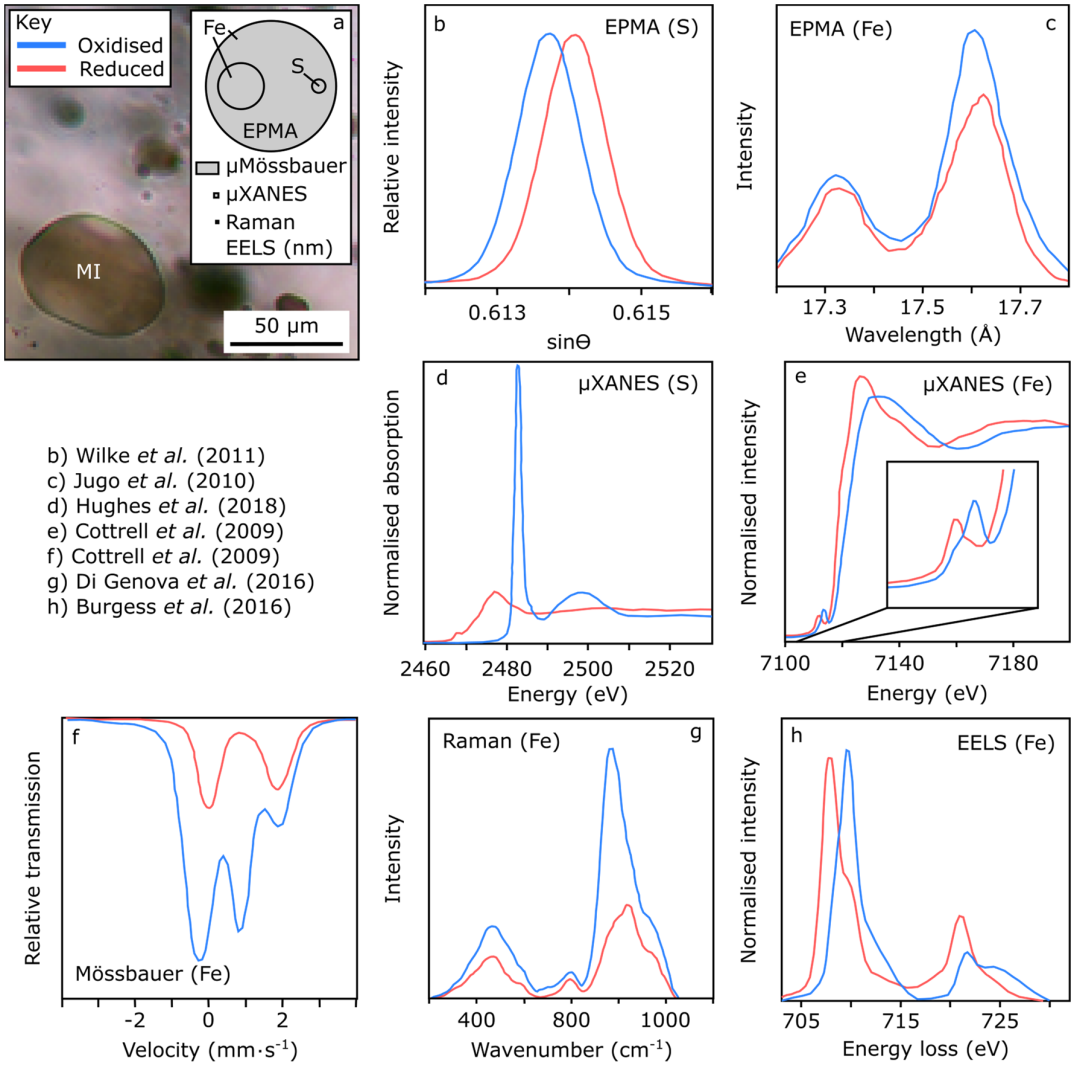

Figure 4. a) Olivine-hosted melt inclusion from Stromboli (Italy) with the spatial resolution of the different techniques shown for comparison. b-h) Example spectra for reduced (red) and oxidised (blue) species, with b and d) S; c and e) to h) Fe using EPMA for b) and c), µ-XANES for d) and e), Mössbauer for f), Raman for g), and EELS for h).

3.1. Electron probe microanalysis (EPMA)

Measuring the Fe oxidation state with EPMA used the X-rays produced by the electron transition from 3d to 2p, which generates the Fe L-lines (Fig. 4c). The change in peak position and intensity of the Fe Lα- and Lβ-peaks are a function of Fe concentration and coordination, but more importantly the oxidation state, which can be calibrated to quantify the Fe^{2+}/FeT ratio [27]. The intensities of the Fe L-peaks increase with increased Fe concentration and for more oxidised samples, whilst the Fe L-peak positions shift to higher wavelengths with increased Fe concentration or for more reduced samples [17]. There are two methods to exploit these changes in the Fe L-peaks: the 'peak shift' or 'flank' method [28]. The peak shift method correlates the

position of the Fe Lα-peak at a given Fe concentration with the Fe^{2+}/FeT [29]. The flank method correlates the change in the intensity ratio of positions on the low wavelength flank of Fe-Lα (Fe-Lαf) and the high wavelength flank of Fe-Lβ (Fe-Lβf) (Fe-Lαf / Fe-Lβf) [28, 30, 31]. The flank method has greater sensitivity than the peak shift method because it utilises both changes in peak position and intensity [28]. Silicate glass standards of similar compositions (e.g., basalt) are required to create calibration curves for each analytical session [17, 18]. Due to beam damage during the time required to perform a meaningful analysis, it is usual to constantly move the sample around to analyse new areas [18]. Alternatively, using a static stage requires using a time-dependent intensity data collection approach (e.g., [32]), which improves spatial resolution (avoiding any heterogeneity) and is essential when glass availability is limited [17]. In a similar way, the shift in the peak position of S-Kα is used to quantify S^{6+}/ST for S oxidation state, requiring similar analytical precautions (Fig. 4b) [25, 33-35].

3.2. Mössbauer spectroscopy

Mössbauer spectroscopy uses the recoil-free resonant absorption of gamma rays to probe changes in the energy levels of an atomic nucleus in response to the surrounding electric and magnetic environment. Gamma rays over a narrow energy range are transmitted through the sample and the resulting absorption spectra gives information on the coordination and oxidation state (Fig. 4f). In conventional Mössbauer spectroscopy for iron (^{57}Fe), a ^{57}Co radioactive source is moved over a range of velocities to produce gamma rays over the required energy range. These gamma rays are difficult to focus and relatively weak, therefore, long measurement times (days) are needed and the resulting spatial resolution is poor. μ-Mössbauer uses synchrotron radiation and a moving iron borate crystal, which gives a focussed, high brilliance gamma source allowing measurements in minutes at a spatial resolution of ~ 5 × 10 μm [20]. It has been demonstrated that μ-Mössbauer on a beamline such the European Synchrotron Radiation Facility causes no damage to silicate glass even for hydrous samples (pers. comm. Valerio Cerantola ID18).

3.3. X-ray absorption near-edge structure (XANES) spectroscopy

μ-XANES is an X-ray absorption spectroscopy (XAS) technique that uses changes in the pre-edge structure of the Fe K-edge (electronic transition from 1s to 3d), which are caused by changes in the Fe concentration, coordination, and oxidation state (Fig. 4e). Broadly, with decreasing Fe^{2+}/FeT, the edge jump and crest move to higher energies and the higher energy pre-edge feature increases (and the lower energy pre-edge feature decreases) in intensity [21]. There are a variety of ways of quantifying the Fe oxidation state from XANES spectra, such as centroid position of the pre-edge features [21] and principal component analysis [36]. Very high precision on Fe^{2+}/FeT can be obtained using well-characterised standards, but data processing must be consistent between different datasets for robust comparison. It has been demonstrated that high photon fluxes can induce changes in the Fe^{2+}/FeT ratio during analysis, especially in hydrous samples [37, 38]. Similar procedures can be used to quantifying the S oxidation state using the S K-edge (Fig. 4d) and oxidation/reduction problems can also occur during these analyses [14, 39].

3.4. Raman spectroscopy

Raman spectroscopy measures the shift in wavelength of monochromatic light due to inelastic scattering of the incident photons when they interact with molecular vibrations, where the electron cloud is deformable. There are various bands sensitive to the Fe oxidation state of silicate glass, which increases in intensity with increasing Fe^{3+} content at constant Fe concentration [22, 23] (Fig. 4g). Both spectral deconvolution [22] and empirical calibrations based on ideal mixing equations [23] have been used to quantify the Fe^{2+}/FeT. The sensitivity of the technique and calibration are composition dependent, with pantelleritic rhyolites being much more sensitive than basalts, and the water content being very important. Uniquely, Raman (in confocal more) can analyse unexposed areas of glass, which means melt inclusions do not have to be exposed at the surface for analysis. It is also possible to damage the glass at high laser power and even induce the formation of nanolites [40].

3.5. Electron energy-loss spectroscopy (EELS)

EELS in an aberration-corrected scanning-transmission electron microscope (TEM) technique, which offers the opportunity to measure the Fe oxidation state at sub-nanometre scale. The Fe L-edge is caused by inner shell 2p electrons being excited to the unoccupied 3d shell and these produce two distinct edges whose shape and position are dependent on the oxidation state, symmetry, and coordination state of the Fe atom [24] (Fig. 4h). Gaussian fits to the spectra could provide a way to quantify the Fe oxidation state but it can prove difficult to find standards that are homogeneous at the scale of analysis, which currently precludes quantification [24]. The high beam energies used for EELS can damage the glass [24].

4. BEAM-INDUCED REDOX CHANGES

Silicate glass can be unstable under electron and photon beams (depending on the analytical conditions), which results in a variety of ways that glasses can change composition and structure during analysis (e.g., [17, 34]). Understanding the redox mechanisms occurring in the glass during analysis (and trying to mitigate them) requires using a variety of techniques to monitor for changes in both composition and structure over time, both syn- and post-irradiation. Electron beam damage has been investigated during EPMA and EELS analysis (e.g., [17, 24]), whilst photon beam damage has been investigated during μ-XANES and Raman spectroscopy (e.g., [38, 40]).

4.1. EPMA

Syn-irradiation measurements of X-ray intensities using EPMA have shown that the concentration of mobile elements (e.g., Na, K) decreases with time, the concentration of immobile elements (e.g., Si, Al) show a concomitant increase with time, and both oxidation and

reduction of Fe and S occur with time (e.g., [17, 18, 25, 32, 35, 41]) (Figs. 5a to 5c). Unfortunately, EPMA is unable to measure the change in light elements (e.g., H and Li) or the formation of nanolites, but these can be measured post-irradiation using alternative techniques. Secondary ion mass spectrometry depth profiles (e.g., H^+ and Li^+) show that mobile elements predominantly show a depletion in concentration within the analysis area and an increase in concentration below the analysis area [42] (Fig. 2f). Raman maps of the analysed area have shown that H_2O concentration decreases and the degree of nanolitisation increases (Figs. 2d and 2e). μ-XANES analysis of the S K-edge have shown the presence of S^{4-} post irradiation, which does not occur in areas not analysed previously using EPMA [34].

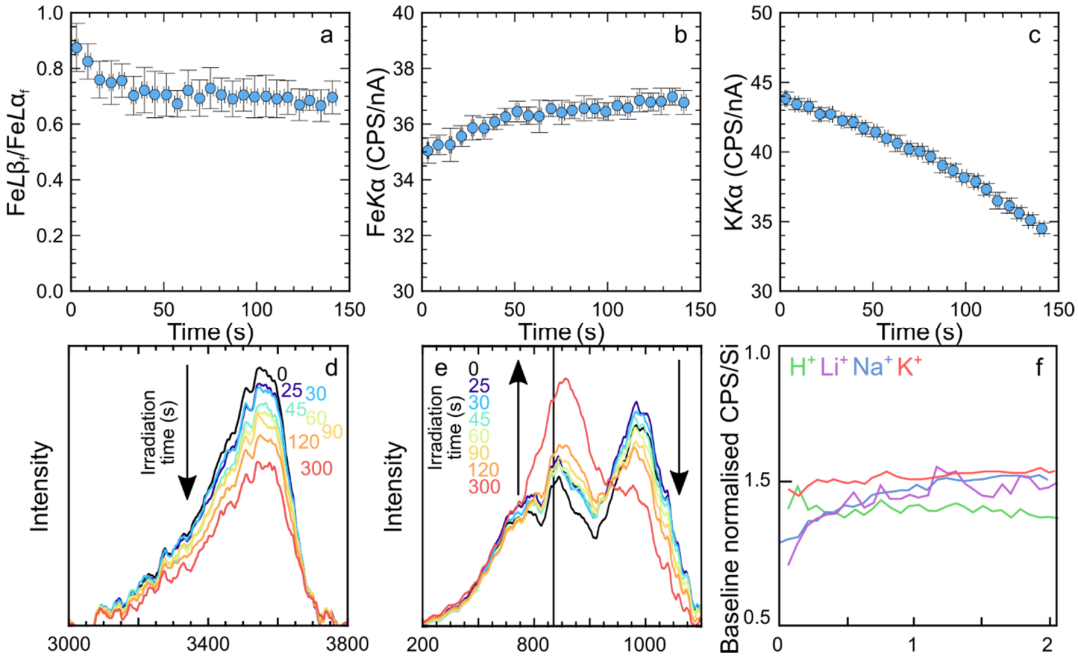

Figure 5. Changes in glass composition and structure during electron beam irradiation: EPMA time-dependent intensity data for a) Fe oxidation state, b) grow-in of an immobile element (Fe), and c) migration of a mobile element (K). Raman data for d) H_2O peak over time, and e) silicate peak region (including magnetite peak indicated by solid, black, vertical line) over time. f) SIMS data for mobile elements from [42].

During EPMA, electrons are trapped within the sample (in the band gap), generating a region of negative charge below the interaction volume, which produces an electric field within the glass [43, 44] (Fig. 6). This causes the mobile, positive ions (e.g., Na^+, H^+, K^+) to migrate towards the region of negative charge, whilst immobile ions remain static and, therefore, their concentration increases. The migration of mobile elements leaves behind oxygen, which can oxidise Fe, eventually precipitating nanolites of magnetite and even haematite or outgassing from the surface of the sample [17, 45]. The rate of oxidation is controlled primarily by the H_2O concentration, with increasing H_2O increasing the oxidation rate [17]. If there are few mobile ions available

(e.g., anhydrous glass), the trapped electrons cause the Fe to reduce, with the rate controlled by the initial Fe oxidation state. High silica glasses do not oxidise, possibly due to their low Fe concentration but interestingly H appears to migrate into the analysis volume implying OH^- rather H^+ migration [17, 42]. The rate of Fe redox changes is additionally controlled by the analytical conditions: decreased beam size, increased beam current, and decreased accelerating voltage all increase the rate of redox change.

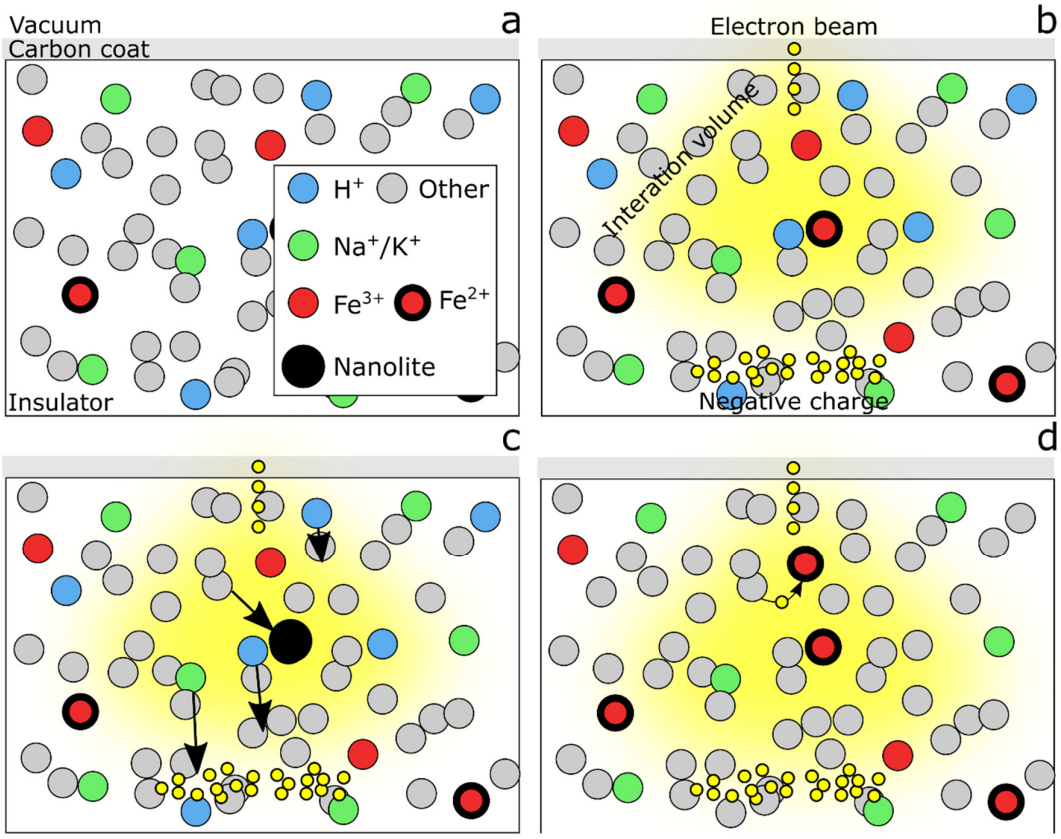

Figure 6. Schematic diagram of the processes occurring during electron beam irradiation during EPMA: a) carbon-coated glass in a vacuum prior to electron beam irradiation containing mobile elements (e.g., H, Na, and K) and variably oxidised Fe (and other glass components such as O, Ca, etc.); b) electron beam irradiation begins, electrons are trapped building up a region of negative charge above which an electric field is present; and c) in hydrous glasses positively charged mobile ions migrate towards the negative charge at depth, oxidising Fe and precipitating nanosized crystals of magnetite; or d) in anhydrous glass electrons are transferred from oxygen to Fe^{3+} causing reduction.

The mechanism for S redox changes are probably similar to Fe, although oxidation proceeds via S^{4+} formation and increases in S^{6+} [34]. Analytical conditions have a similar effect as for Fe, with oxidation rate increasing with increased acquisition time or decreasing beam size [25, 35]. Oxidation occurs for initially reduced glass, whilst reduction can occur for initially oxidised

glasses, and low S concentration glasses are particularly affected [25, 41]. Extremely rapid oxidation has been observed for very S-rich glasses, but this may have been because they were Fe-free, hence Fe-bearing glasses may be less sensitive to beam damage [39, 46].

4.2. EELS

During EELS analysis, the concentration of most elements except Si decreases in the analysed region (using EDS) and the Fe oxidation state changes (using EELS) [24]. Magnetite nanolites were also observed in the glass, but it is not certain whether these were present before analysis [24]. These observations illustrate that the damage is caused by an electric field in the glass, but due to a different mechanisms than during EPMA. For EELS, as the sample is very thin, the emission of secondary and auger electrons generates a region of positive charge in the analysis area, generating an electric field [24, 43]. This region of positive charge causes the cations to migrate out of the analysis area, reducing their concentration in the area and causing oxidation [24]. There is no clear relationship between sample thickness, electron dose rate or total dose with rate of oxidation change [24]. Generally reduced samples become more oxidised with increasing dose and that at the highest doses the oxidation state reduces [24]. Additionally, during sample preparation and loading into the microscope, surface oxidation occurs: initially oxidised samples have a thinner layer as there is less of driving force for oxidation [24].

4.3. XANES

Time-dependent measurements at a single energy (e.g., the second pre-edge multiplet) or repeated measurements on the same spot during μ-XANES can be used to monitor beam damage. These measurements on the Fe K-edge for anhydrous basaltic glass and anhydrous to hydrous dacitic to rhyolitic glass show no change in oxidation state with time [21, 36, 47, 48]. On hydrous basaltic glass, the Fe^{3+} multiplet increases in intensity, the Fe^{2+} multiplet decreases, and the white line shifts to higher energy, which implies oxidation of Fe^{2+} to Fe^{3+} rather than increased 3d-4p hybridisation [38]. Oxidation is faster at higher photon fluxes, cryogenic temperatures, higher H_2O concentrations or more reduced samples, and was permanent [38]. FTIR spectra of the analysed area showed a reduction in H_2O concentration [38]. On the other hand, glasses with low Fe concentrations (< 5,000 ppm Fe) show reduction over time but the Fe coordination did not change [37]. The rate of reduction increases with decreasing Fe content and the absolute amount of Fe reduced was the same regardless of the total Fe content [37]. After irradiation, the glass had grey marks, which are usually associated with anionic vacancies associated with cationic displacement [37]. The reduction could be reversed by heating the sample and conducting the measurements at higher temperatures (450 - 500 °C) prevented oxidation [37].

The data for S are more complicated, as different beam lines appear to produce different results, likely due to their different beam intensities [39]. Initially oxidised glasses reduce over time and S^{4-} is observed, with the rate controlled by the beam conditions and increases with H_2O present, whilst partially/completely reduced sample do not change speciation [34, 39]. On the other hand,

oxidation is seen at higher intensity beam lines especially with H_2O present [34]. Sulphur becomes more stable with increasing S/Fe ratio [46].

The mechanism proposed for both Fe and S oxidation involves H_2O [38, 46]:

$$2Fe^{2+}O(glass) + H_2O(glass) \rightarrow Fe^{3+}{}_2O_3 + H_2(gas)$$

$$S^{2-}(glass) + 4H_2O(glass) \rightarrow SO_4{}^{2-}(glass) + 4H_2(gas)$$

The photon radiation breaks the O–H bonds, then H outgases from the sample leaving behind O to oxidise S or Fe. The increased rate of oxidation observed at cryogenic temperature for Fe maybe that O cannot diffuse at such low temperatures and hence oxidation is increased [38]. Conversely, Fe reduction is thought to occur because the X-ray beam creates defects in the glass, which provide the charge to convert Fe^{3+} to Fe^{2+}, and increased temperature relaxes these defects [37].

4.4. Raman

During Raman spectroscopy, the band associated with the Fe^{3+} peak (~970 cm^{-1}) has been seen to increase, where the change increased with increasing acquisition time or at higher laser powers, and there was a decrease in intensity of the H_2O peak [40]. The change was more prominent in alkali-rich or Fe-rich samples [41]. This is thought to be due to laser heating causing the same reaction to occur as for μ-XANES [40]. Nonetheless, both the sample oxidation and water loss can be avoided when using a laser power less than 5 mW and acquisition times lower than ~ 3 minutes (see [40] for more details).

5. CONCLUSION

Irradiation using an electron (EPMA or EELS) or photon (XANES or Raman) beam can cause reduction or oxidation of silicate glass. The rate and direction of redox change depends on the analytical conditions (e.g., accelerating voltage, beam current, photon flux, laser power, etc.) and measurement time, but also on the glass composition (e.g., silica, Fe, and H_2O concentrations). For XANES Fe-poor glasses reduce whilst Fe-rich glasses oxidise, whereas for EPMA alkali-poor anhydrous glasses reduce whilst alkali-rich hydrous glasses oxidise. Broadly, increased H_2O, alkali-content or Fe increases the rate of redox change with both electron and photon beams, although higher Fe contents appear to stabilise the oxidation state of S. Oxidation is caused by cation mobilisation, either due to addition/removal of electrons, photon induced bond breaking or heating. Careful consideration of analytical conditions can allow the glass to be analysed multiple times using a variety of techniques to fully characterise silicate glass samples.

6. REFERENCES

[1] Kress V C and Carmichael I S E 1991 *Contrib. Mineral. Petrol.* **108** 82-92
[2] Wilke M 2005 *Ann. Geophys.* **48** 609-617
[3] Vicenzi E P, *et al.* 1994 *Chem. Geol.* **117** 355-360
[4] Tattitch B and Blundy J 2017 *Appl. Earth Sci.* **126**
[5] Cukierman M and Uhlmann D R 1974 *J. Geophys. Res.* **79** 1594-1598
[6] Dingwell D B and Virgo D 1987 *Geochim. Cosmochim. Acta* **51** 195-205
[7] Hamilton D L, *et al.* 1964 *J. Petrology* **5** 21-39
[8] Carmichael I S E and Ghiorso M S 1990 *Rev. Mineral. Geochem.* **24** 191-212
[9] Bouhifd M A, *et al.* 2004 *Earth Planet. Sci. Lett.* **218** 31-44
[10] Humphreys M C S, *et al.* 2015 *J. Petrology* **56** 795-814
[11] Kelley K A and Cottrell E 2009 *Science* **325** 605-607
[12] Mujin M, *et al.* 2017 *Amer. Mineralogist* **102** 2367-2380
[13] Di Genova D, *et al.* 2018 *Lithos* **318-319** 209-218
[14] Jugo P J, *et al.* 2010 *Geochim. Cosmochim. Acta* **74** 5926-5938
[15] Roedder E 1979 *Bull. Mineral.* **102** 487-510
[16] McCammon C A 1999 in: *Proc. VIIth Int. Kimberlite Conference*. 540-544
[17] Hughes E C, *et al.* 2018 *Amer. Mineralogist* **103** 1473-1486
[18] Zhang C, *et al.* 2018 *Amer. Mineralogist* **103** 1445-1454
[19] Fialin M, *et al.* 2001 *Amer. Mineralogist* **86** 456-465
[20] Potapkin V, *et al.* 2012 *J. Synchrotron Rad.* **19** 559-569
[21] Cottrell E, *et al.* 2009 *Chem. Geol.* **268** 167-179
[22] Di Muro A, *et al.* 2009 *Chem. Geol.* **259** 78-88
[23] Di Genova D, *et al.* 2016 *Amer. Mineralogist* **101** 943-952
[24] Burgess K D, *et al.* 2016 *Amer. Mineralogist* **101** 2677-2688
[25] Rowe M C, *et al.* 2007 *Chem. Geol.* **236** 303-322
[26] Bonnin-Mosbah M, *et al.* 2002 *Spectrochim. Acta B: At. Spectrosc.* **57** 711-725
[27] Gopon P, *et al.* 2013 *Microsc. Microanal.* **19** 1698-1708
[28] Hofer H E, *et al.* 1994 *Eur. J. Mineralogy* **6** 407-418
[29] Fialin M, *et al.* 2004 *Amer. Mineralogist* **89**
[30] Hofer H E 2002 *Mössbauer Spectrosc.* **144/145** 239-248
[31] Hofer H E and Brey G P 2007 *Amer. Mineralogist* **92** 873-885
[32] Nielsen C H and Sigurdsson H 1981 *Amer. Mineralogist* **66** 547-552
[33] Wallace P and Carmichael I S E 1992 *Geochim. Cosmochim. Acta* **56** 1863-1874
[34] Wilke M, *et al.* 2008 *Amer. Mineralogist* **93**
[35] Metrich N and Clocchiatti R 1996 *Geochim. Cosmochim. Acta* **60** 4151-4160
[36] Shorttle O, *et al.* 2015 *Earth Planet. Sci. Lett.* **427** 272-285
[37] Gonçalves Ferreira P, *et al.* 2013 *Chem. Geol.* **346** 106-112
[38] Cottrell E, *et al.* 2018 *Amer. Mineralogist* **103** 489-501
[39] Wilke M, *et al.* 2011 *Rev. Mineral. Geochem.* **73** 41-78
[40] Di Genova D, *et al.* 2017 *Chem. Geol.* **475** 76-86

[41] Jugo P J, *et al.* 2005 *Geochim. Cosmochim. Acta* **69** 497-503
[42] Humphreys M C S, *et al.* 2006 *Amer. Mineralogist* **91** 667-679
[43] Cazaux J 1996 *X-ray Spectrom.* **25** 265-280
[44] Bonnelle C 2004 *Microsc. Microanal.* **10** 691-696
[45] Fialin M and Wagner C 2012 *J. Non. Cryst. Solids* **358** 1617-1623
[46] Klimm K, *et al.* 2012 *Chem. Geol.* **322-323** 237-249
[47] Moussallam Y, *et al.* 2014 *Earth Planet. Sci. Lett.* **393** 200-209
[48] Fiege A, *et al.* 2017 *Amer. Mineralogist* **102** 369-380